

Electronic Supplementary Information for Glutathione Displacement Assay Based on Fluorescent Au(I) Complex

Shinae Lee,^{a,b} Seunga Heo,^b Jihwan Park,^c Jeongyun Heo,^{c} Sehoon Kim,^{c,d*} and Youngmin You^{a*}*

^a Department of Chemical and Biomolecular Engineering, Yonsei University, Seoul 03722, Republic of Korea.

^b Division of Chemical Engineering and Materials Science, Ewha Womans University, Seoul 03760, Republic of Korea.

^c Chemical and Biological Integrative Research Center, Korea Institute of Science and Technology, Seoul 02792, Republic of Korea.

^d KU-KIST Graduate School of Converging Science and Technology, Korea University, Seoul 02841, Republic of Korea.

e-mail: kyunheo@kist.re.kr; sehoonkim@kist.re.kr; odds2@yonsei.ac.kr

CONTENTS

Table S1.	Calculated electronic transition energies of [Au(BZI) ₂] ⁺
Table S2.	Cartesian coordinates for the optimized geometry of [Au(BZI) ₂] ⁺
Table S3.	Calculated electronic transition energies of [Au(BZI)(SCH ₃)], the truncated model for [Au(BZI)(GS)]
Table S4.	Cartesian coordinates for the optimized geometry of [Au(BZI) ₂] ⁺
Fig. S1	Photoluminescence responses of 20 μM [Au(BZI) ₂] ⁺ to 2.0 mM GSH in an aqueous solution of 100 mM KCl, with no DMSO present
Fig. S2	Determination of the limit of detection (LOD) of the fluorescence response of [Au(BZI) ₂] ⁺ for GSH
Fig. S3	Photoluminescence responses of 20 μM [Au(BZI) ₂] ⁺ to 2.0 mM GSH in an aqueous solution containing 100 mM KCl at various pHs (4.3–10.3)
Fig. S4	Mass spectra (positive mode, ESI) recorded for 0.10 mM [Au(BZI) ₂] ⁺ in the absence and

the presence of 50 mM GSH

- Fig. S5** Simulated electronic transition spectra of $[\text{Au}(\text{BZI})_2]^+$ and the truncated model for $[\text{Au}(\text{BZI})(\text{GS})]$, $[\text{Au}(\text{BZI})(\text{SCH}_3)]$
- Fig. S6** Photoluminescence decays of 20 μM $[\text{Au}(\text{BZI})_2]^+$ dissolved in a buffered aqueous solution (pH 7.4; 25 mM PIPES, 100 mM KCl, and 60 vol% DMSO) in the absence and presence of 4.0 mM GSH recorded at 489 nm after pulsed laser photoexcitation of 377 nm (temporal resolution = 50 ps)
- Fig. S7** Senescence-associated β -galactosidase (SA- β -gal) stained images of (a) normal and (b) senescent preadipocytes. (c) Quantitative comparison of the SA- β -gal-stained areas from images of (a) and (b)
- Fig. S8** Cytotoxicity of $[\text{Au}(\text{BZI})_2]^+$ against HeLa cells, evaluated by the colorimetric WST-8 assay
- Fig. S9** Photoluminescence co-localization image of senescent preadipocytes stained with $[\text{Au}(\text{BZI})_2]^+$ and MitoTracker
- Fig. S10** FACS analysis data for (a) normal and (b) senescent preadipocytes treated with 1 μM $[\text{Au}(\text{BZI})_2]^+$
- Fig. S11** Photoluminescence micrographs of normal preadipocytes (a) without and (b) with pre-treatment with 1.0 μM N-ethylmaleimide. The both cells were subsequently incubated with 0.10 μM $[\text{Au}(\text{BZI})_2]^+$ for 36 h. (c) Comparison of the photoluminescence intensities of panels (a) and (b)
- Fig. S12** Comparison of total GSH concentrations of normal and senescent preadipocytes determined using a colorimetric ELISA technique. (a) Total GSH concentration obtained from the lysate of 1.0×10^5 normal and senescent preadipocytes. (b) Calibration curve between the absorbance at a wavelength of 405 nm and the total GSH concentration of the cell lysate
- Fig. S13** ^1H NMR spectrum (300 MHz, CD_2Cl_2) of **1**
- Fig. S14** $^{13}\text{C}\{^1\text{H}\}$ NMR spectrum (126 MHz, CD_2Cl_2) of **1**
- Fig. S15** High-resolution mass spectrum (EI, positive) of **1**
- Fig. S16** ^1H NMR spectrum (300 MHz, CD_2Cl_2) of **2**
- Fig. S17** $^{13}\text{C}\{^1\text{H}\}$ NMR spectrum (126 MHz, CD_2Cl_2) of **2**
- Fig. S18** High-resolution mass spectrum (FAB, positive) of **2**
- Fig. S19** ^1H NMR spectrum (300 MHz, CD_2Cl_2) of $[\text{Au}(\text{BZI})_2]\text{Cl}$
- Fig. S20** $^{13}\text{C}\{^1\text{H}\}$ NMR spectrum (126 MHz, CD_2Cl_2) of $[\text{Au}(\text{BZI})_2]\text{Cl}$
- Fig. S21** High-resolution mass spectrum (FAB, positive) of $[\text{Au}(\text{BZI})_2]\text{Cl}$
- Fig. S22** ^1H NMR spectrum (300 MHz, CD_2Cl_2) of **3**

- Fig. S23** ^1H NMR spectrum (300 MHz, CD_2Cl_2) of $[\text{Au}(\text{BZI})(\text{PhS})]$
- Fig. S24** $^{13}\text{C}\{^1\text{H}\}$ NMR spectrum (126 MHz, CD_2Cl_2) of $[\text{Au}(\text{BZI})(\text{PhS})]$
- Fig. S25** High-resolution mass spectrum (FAB, positive) of $[\text{Au}(\text{BZI})(\text{PhS})]$
-

Table S1. Calculated electronic transition energies of $[\text{Au}(\text{BZI})_2]^+$

state	energy (eV)	participating molecular orbitals (expansion coefficient)	transition character
T_1	3.49	HOMO-1 \rightarrow LUMO (0.25) HOMO \rightarrow LUMO+1 (0.30)	LE
S_1	4.31	HOMO-1 \rightarrow LUMO (0.64)	LE

Table S2. Cartesian coordinates for the optimized geometry of $[\text{Au}(\text{BZI})_2]^+$

Center Number	Atomic Number	Atomic Type	Coordinates (Angstroms)		
			X	Y	Z
1	6	0	2.067289	-0.000006	-0.000019
2	6	0	4.216101	0.694360	0.084467
3	6	0	5.402045	1.418301	0.190922
4	1	0	5.398607	2.500611	0.341728
5	6	0	6.585508	0.696197	0.097780
6	1	0	7.539647	1.223312	0.176160
7	6	0	6.585698	-0.695083	-0.097519
8	1	0	7.539986	-1.221932	-0.175848
9	6	0	5.402417	-1.417491	-0.190729
10	1	0	5.399247	-2.499799	-0.341535
11	6	0	4.216299	-0.693848	-0.084269
12	6	0	2.419292	2.423795	0.300479
13	6	0	2.815172	3.401772	-0.611118
14	6	0	2.394581	4.716519	-0.426517
15	1	0	2.710272	5.489295	-1.132568
16	6	0	1.571295	5.043074	0.649169
17	1	0	1.244491	6.076844	0.792359
18	6	0	1.168503	4.056318	1.547155
19	1	0	0.525480	4.312581	2.393531

20	6	0	1.600197	2.743495	1.383399
21	6	0	2.419720	-2.423626	-0.300534
22	6	0	2.815770	-3.401617	0.610975
23	6	0	2.395231	-4.716383	0.426395
24	1	0	2.711049	-5.489156	1.132389
25	6	0	1.571799	-5.042943	-0.649179
26	1	0	1.245028	-6.076726	-0.792363
27	6	0	1.168845	-4.056166	-1.547069
28	1	0	0.525713	-4.312434	-2.393363
29	6	0	1.600502	-2.743328	-1.383351
30	7	0	2.873896	1.080193	0.127143
31	7	0	2.874154	-1.079972	-0.127085
32	79	0	0.000002	-0.000061	-0.000179
33	1	0	3.448619	3.127786	-1.460210
34	1	0	3.449260	-3.127617	1.460029
35	1	0	1.319492	-1.964122	-2.098002
36	1	0	1.319360	1.964270	2.098098
37	6	0	-2.067275	-0.000105	-0.000090
38	6	0	-4.216243	0.693845	-0.084214
39	6	0	-5.402312	1.417605	-0.190676
40	6	0	-4.216140	-0.694358	0.084483
41	6	0	-5.402144	-1.418211	0.190798
42	6	0	-6.585649	0.695302	-0.097564
43	1	0	-7.539918	1.222179	-0.175898
44	6	0	-6.585535	-0.696001	0.097639
45	1	0	-7.539691	-1.223109	0.175910
46	1	0	-5.398929	2.499910	-0.341480
47	1	0	-5.398875	-2.500539	0.341510
48	7	0	-2.874093	1.079967	-0.127034
49	7	0	-2.873918	-1.080238	0.127128
50	6	0	-2.419280	-2.423809	0.300556
51	6	0	-2.815132	-3.401870	-0.610957
52	6	0	-1.600141	-2.743454	1.383456
53	6	0	-2.394459	-4.716589	-0.426340

54	1	0	-3.448700	-3.128032	-1.460009
55	6	0	-1.168339	-4.056236	1.547226
56	1	0	-1.319259	-1.964225	2.098137
57	6	0	-1.571083	-5.043071	0.649300
58	1	0	-2.710184	-5.489362	-1.132382
59	1	0	-0.525257	-4.312384	2.393596
60	1	0	-1.244217	-6.076811	0.792546
61	6	0	-2.419744	2.423651	-0.300427
62	6	0	-1.600663	2.743435	-1.383340
63	6	0	-2.815711	3.401560	0.611203
64	6	0	-1.169129	4.056301	-1.547075
65	1	0	-1.319787	1.964252	-2.098064
66	6	0	-2.395284	4.716369	0.426598
67	1	0	-3.448973	3.127451	1.460384
68	6	0	-1.572053	5.043015	-0.649095
69	1	0	-0.526097	4.312654	-2.393419
70	1	0	-2.711065	5.489134	1.132617
71	1	0	-1.245378	6.076828	-0.792283

Table S3. Calculated electronic transition energies of [Au(BZI)(SCH₃)], the truncated model for [Au(BZI)(GS)]

state	energy (eV)	participating molecular orbitals (expansion coefficient)	transition character
T ₁	3.32	HOMO → LUMO (0.68)	XLCT
S ₁	3.59	HOMO → LUMO (0.70)	XLCT

Table S4. Cartesian coordinates for the optimized geometry of [Au(BZI)(SCH₃)]

Center Number	Atomic Number	Atomic Type	Coordinates (Angstroms)		
			X	Y	Z
1	6	0	-0.417888	0.362247	-0.000776
2	6	0	-2.311764	1.614782	-0.012458
3	6	0	-3.620843	2.087891	0.006160
4	1	0	-4.471201	1.402239	0.041611
5	6	0	-3.794627	3.468623	-0.020859
6	1	0	-4.807562	3.879626	-0.007380
7	6	0	-2.699407	4.343314	-0.067374
8	1	0	-2.876609	5.421671	-0.097270
9	6	0	-1.390758	3.869183	-0.073107
10	1	0	-0.533826	4.546781	-0.107019
11	6	0	-1.218208	2.488115	-0.033869
12	6	0	-2.553757	-0.871488	0.038356
13	6	0	-3.493217	-1.109352	-0.964425
14	6	0	-4.252184	-2.276013	-0.928434
15	1	0	-4.986345	-2.468112	-1.715569
16	6	0	-4.062502	-3.202858	0.094446
17	1	0	-4.653321	-4.122608	0.114755
18	6	0	-3.115390	-2.960988	1.087521
19	1	0	-2.960420	-3.688411	1.888551

20	6	0	-2.362174	-1.791044	1.068488
21	6	0	1.262569	2.164990	-0.026199
22	6	0	1.680982	3.030630	0.983675
23	6	0	2.995864	3.488738	0.992448
24	1	0	3.328250	4.163105	1.786317
25	6	0	3.888631	3.072182	0.007247
26	1	0	4.923516	3.424614	0.023122
27	6	0	3.463631	2.203156	-0.995915
28	1	0	4.161758	1.873089	-1.769793
29	6	0	2.147206	1.752639	-1.022728
30	7	0	-1.778359	0.325137	0.004048
31	7	0	-0.079480	1.681941	-0.024019
32	79	0	0.903404	-1.212979	0.006843
33	1	0	-3.611302	-0.386773	-1.777537
34	1	0	0.978606	3.324125	1.769675
35	1	0	1.798196	1.075407	-1.807454
36	1	0	-1.618066	-1.585244	1.842958
37	16	0	2.432547	-2.970610	-0.002510
38	6	0	4.013863	-2.054447	-0.138820
39	1	0	4.175555	-1.371995	0.710613
40	1	0	4.831363	-2.792589	-0.144498
41	1	0	4.076437	-1.471192	-1.072028

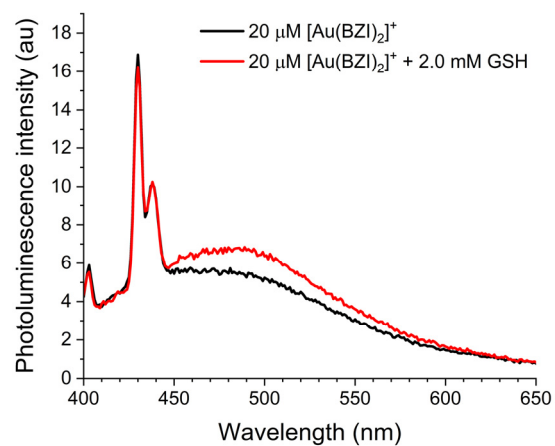


Fig. S1 Photoluminescence responses of 20 μM $[\text{Au}(\text{BZI})_2]^+$ to 2.0 mM GSH in an aqueous solution of 100 mM KCl, with no DMSO present.

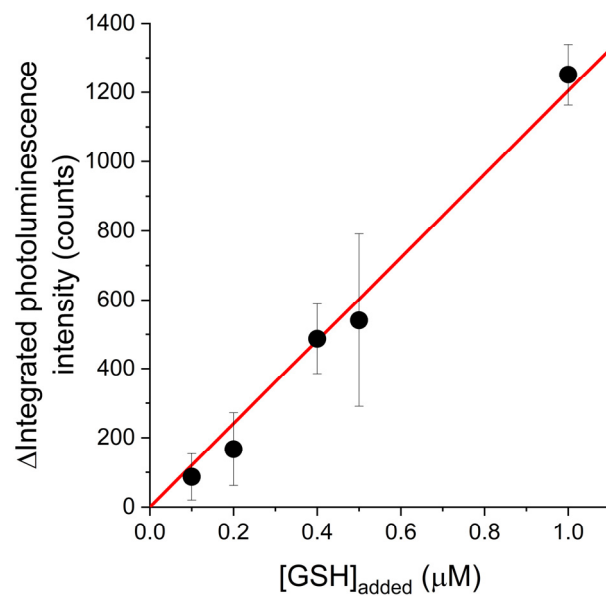


Fig. S2 Determination of the limit of detection (LOD) of the fluorescence response of $[\text{Au}(\text{BZI})_2]^+$ for GSH. LOD was estimated as being $3\sigma/k$, in which σ is the standard deviation for the value obtained after three measurements, and k is the slope shown in the figure.

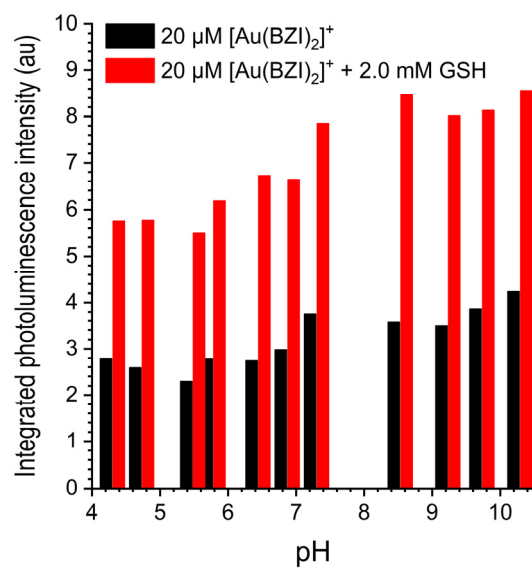


Fig. S3 Photoluminescence responses of 20 μM [Au(BZI)₂]⁺ to 2.0 mM GSH in an aqueous solution containing 100 mM KCl at various pHs (4.3–10.3). The black and red bars are integrated photoluminescence intensities before and after, respectively, the addition of GSH.

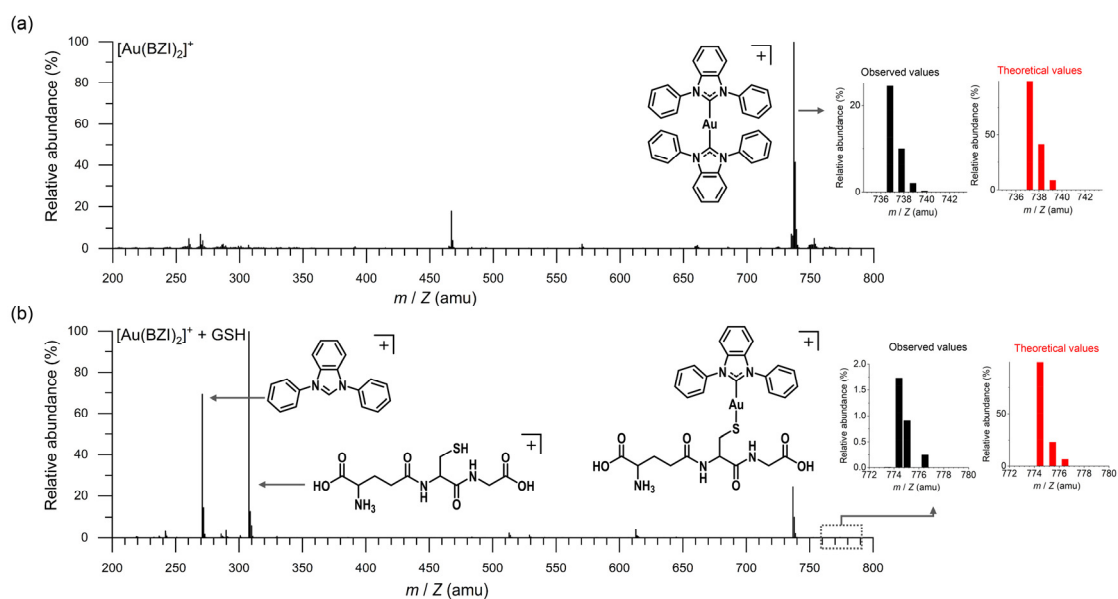


Fig. S4 Mass spectra (positive mode, ESI) recorded for 0.10 mM $[\text{Au}(\text{BZI})_2]^+$ in the (a) absence and (b) presence of 50 mM GSH. The inset graphs show the magnified views (black bars) and the theoretical values (red bars) of the mass-to-charge ratios corresponding to the indicated structures.

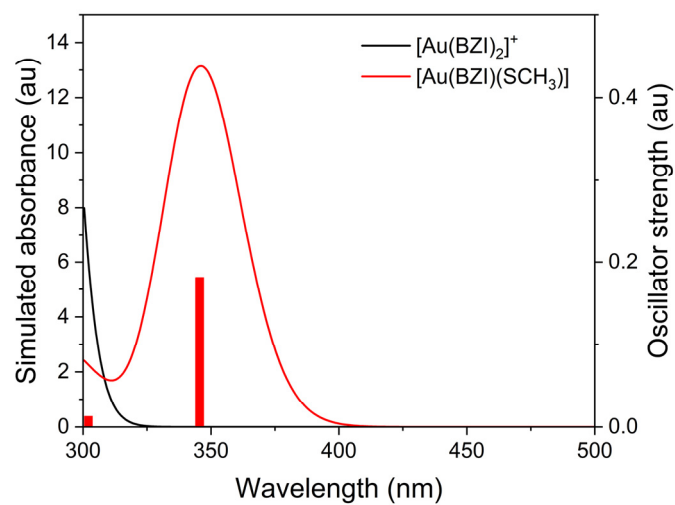


Fig. S5 Simulated electronic transition spectra of $[\text{Au}(\text{BZI})_2]^+$ (black) and the truncated model for $[\text{Au}(\text{BZI})(\text{GS})]$, $[\text{Au}(\text{BZI})(\text{SCH}_3)]$ (red). Bars indicate the calculated oscillator strengths.

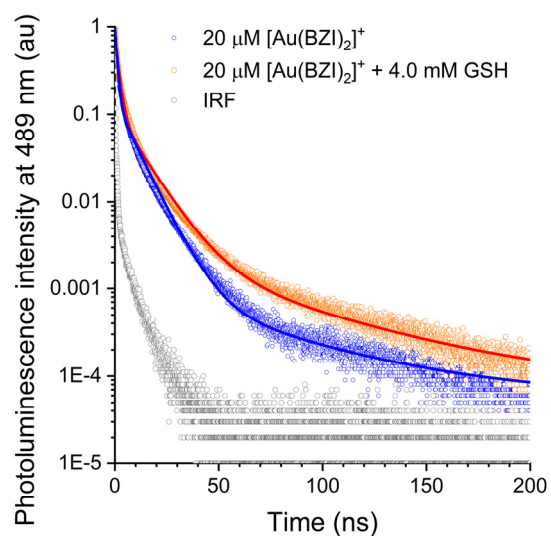


Fig. S6 Photoluminescence decays of $20 \mu\text{M} [\text{Au}(\text{BZI})_2]^+$ dissolved in a buffered aqueous solution (pH 7.4; 25 mM PIPES, 100 mM KCl, and 60 vol% DMSO) in the absence (orange) and presence (blue) of 4.0 mM GSH recorded at 489 nm after pulsed laser photoexcitation of 377 nm (temporal resolution = 50 ps). The solid curves are nonlinear least-squares fits of the transient photoluminescence to a triexponential decay model. Grey symbols are instrumental response function (IRF).

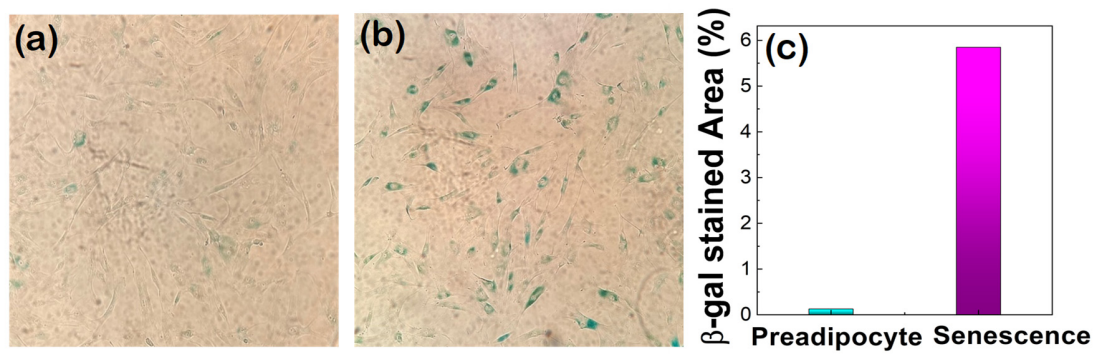


Fig. S7 Senescence-associated β -galactosidase (SA- β -gal) stain images of (a) normal and (b) senescent preadipocytes. (c) Quantitative comparison of the SA- β -gal stained areas from the images of (a) and (b).

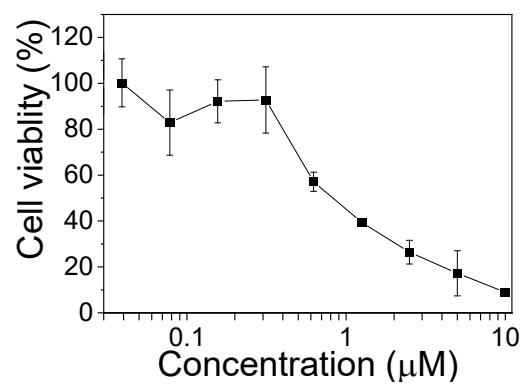


Fig. S8 Cytotoxicity of $[\text{Au}(\text{BZI})_2]^+$ against HeLa cells, evaluated by the colorimetric WST-8 assay. Cells were incubated with varied concentrations of $[\text{Au}(\text{BZI})_2]^+$ in the range 0–10 μM for 48 h. Note that a concentration of 0.10 μM $[\text{Au}(\text{BZI})_2]^+$ was used for our GSH imaging experiments.

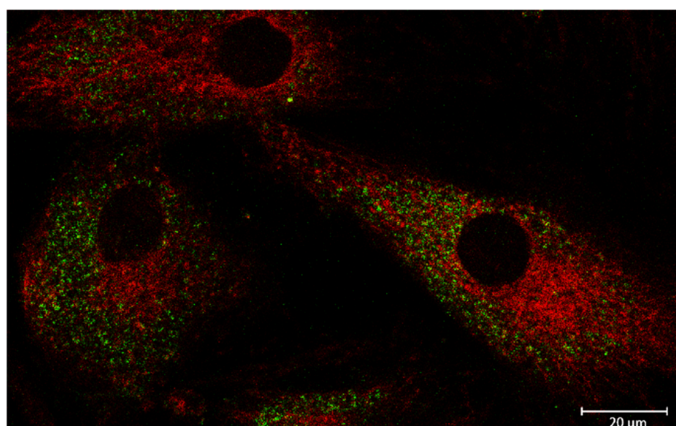


Fig. S9 Photoluminescence co-localization image of senescent preadipocytes stained with [Au(BZI)₂]⁺ (green) and MitoTracker (red).

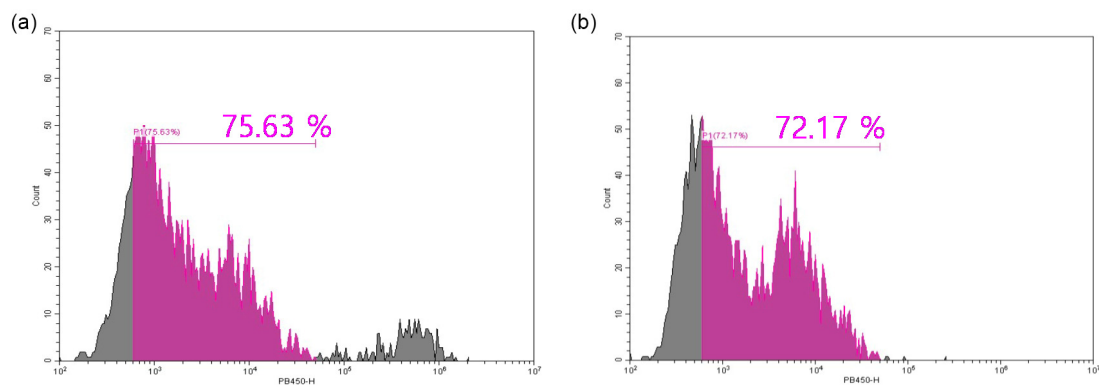


Fig. S10 FACS analysis data for (a) normal and (b) senescent preadipocytes treated with 1 μ M [Au(BZI)₂]⁺.

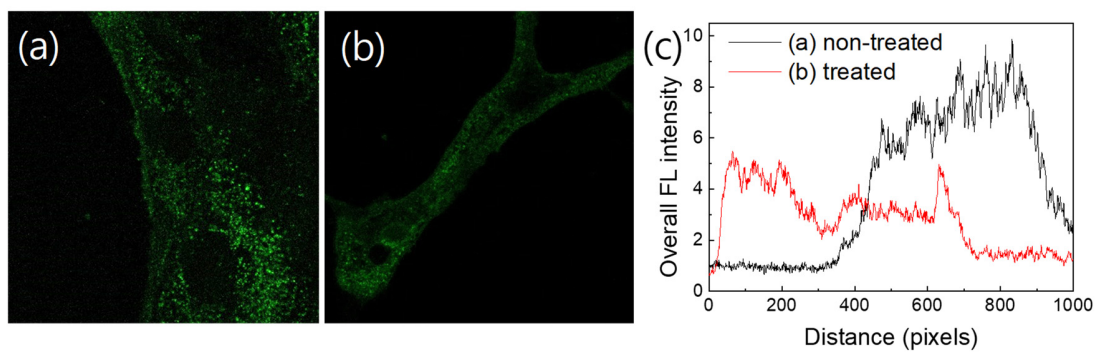


Fig. S11 Photoluminescence micrographs of normal preadipocytes (a) without and (b) with pre-treatment with 1.0 μM *N*-ethylmaleimide. The both cells were subsequently incubated with 0.10 μM $[\text{Au}(\text{BZI})_2]^+$ for 36 h. (c) Comparison of the photoluminescence intensities of panels (a) and (b).

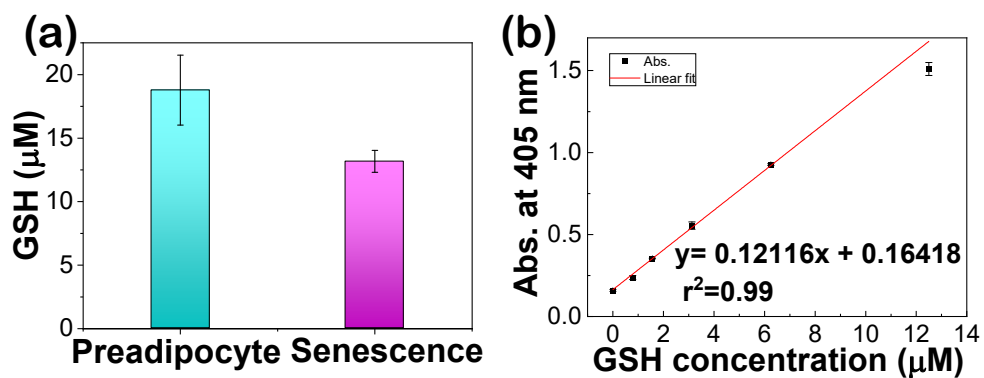


Fig. S12 Comparison of total GSH concentrations of normal and senescent preadipocytes determined using a colorimetric ELISA technique. (a) Total GSH concentration obtained from the lysate of 1.0×10^5 normal (cyan bar) and senescent preadipocytes (pink bar). (b) Calibration curve between the absorbance at a wavelength of 405 nm and the total GSH concentration of the cell lysate.

ISA_C-N_BZI_CD2Cl2 (Dec 27 2021)

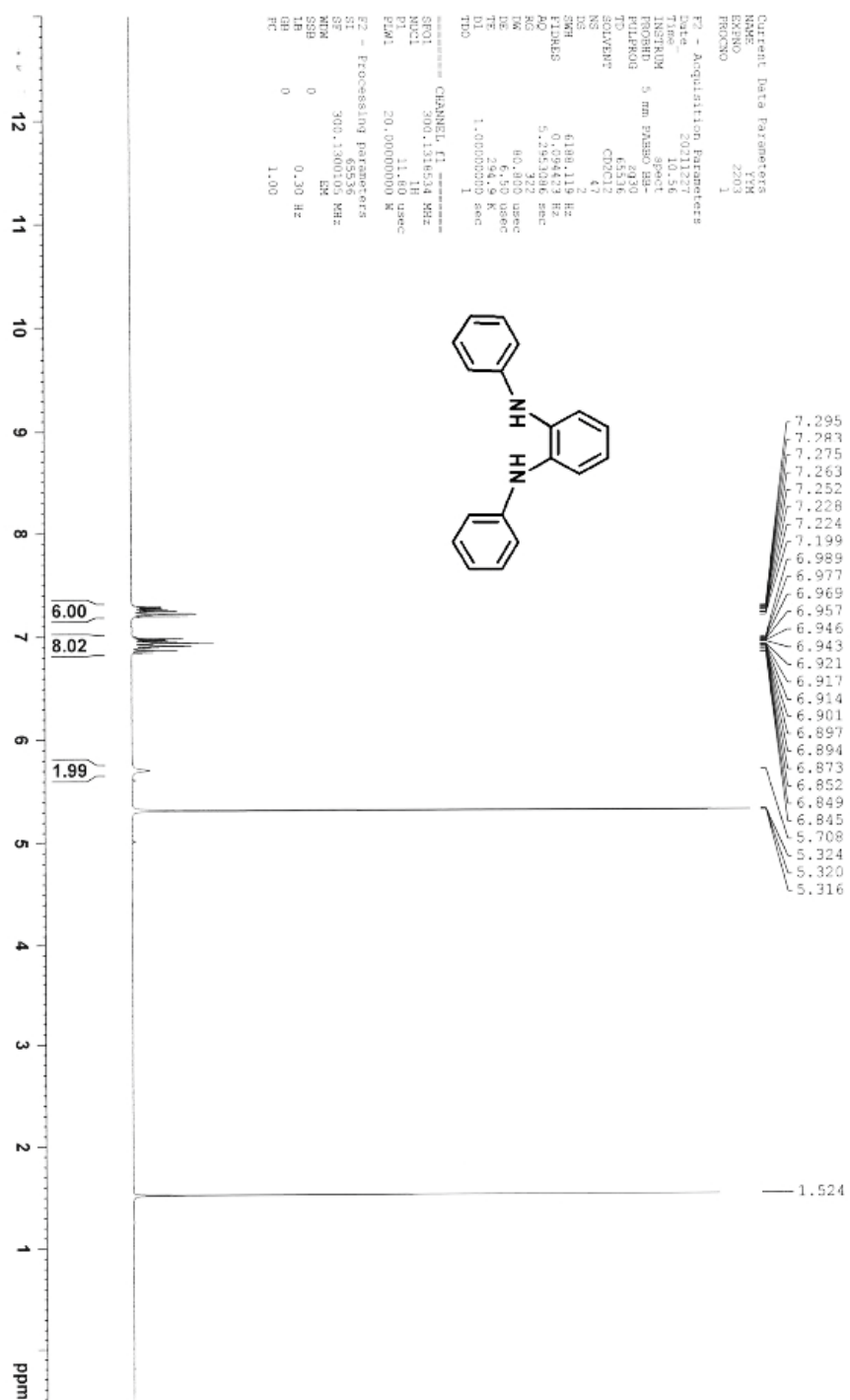
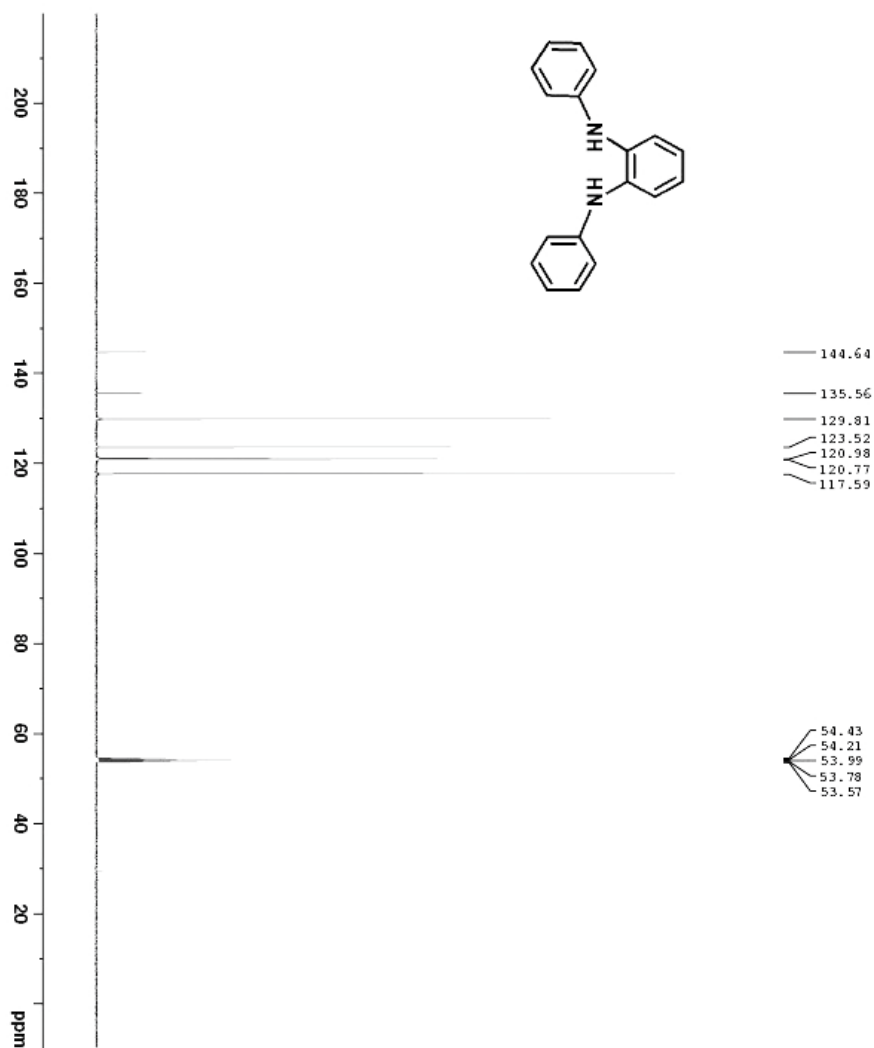


Fig. S13 ¹H NMR spectrum (300 MHz, CD₂Cl₂) of 1.



```

Current Data Parameters
NAME          2d204-wm-1a1
EXPNO         1
PROCNO        1
F2 - Acquisition Parameters
Date_         20220204
Time          17.53 h
INSTRUM      spect
PROBHD       5mmQNP1H1
PULPROG      zgpg30
TD           32768
SOLVENT      CDCl2
NS           1024
DS           4
SWH          31250.000 Hz
FIDRES       1.907349 Hz
AQ           0.5242890 sec
RG           16.000
AQ           1.200 usec
DE           16.000 usec
DM           6.50 usec
TE           298.0 K
D1           2.00000000 sec
D11          0.03000000 sec
TD0          1
SFO1         125.7716224 MHz
NUC1         13C
NUC2         13C usec
PCPD1        90.00000000 M
SFO2         500.1320003 MHz
NUC2         1H
CPDPRG2     waltz16
PCPD2        80.00 usec
PLM2         19.00000000 M
PLM12        0.30686999 M
F2 - Processing parameters
SI           32768
SF           125.757190 MHz
WDW          EM
SSB          0
GB           0
PC           1.40
  
```

Fig. S14 $^{13}\text{C}\{^1\text{H}\}$ NMR spectrum (126 MHz, CD_2Cl_2) of 1.

[Mass Spectrum]
Data : EI-B610 Date : 08-Feb-2022 11:15
RT : 0.15 min Scan#: (5,7)
Elements : C 100/0, H 100/0, N 10/0
Mass Tolerance : 10ppm, 5mmu if m/z < 500, 10mmu if m/z > 1000
Unsaturation (U.S.) : 5.0 - 30.0

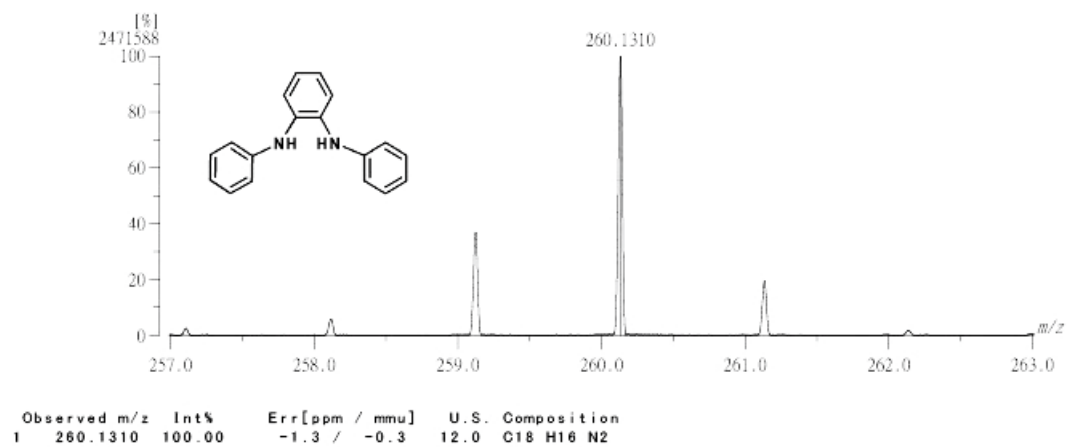


Fig. S15 High-resolution mass spectrum (EI, positive) of 1.

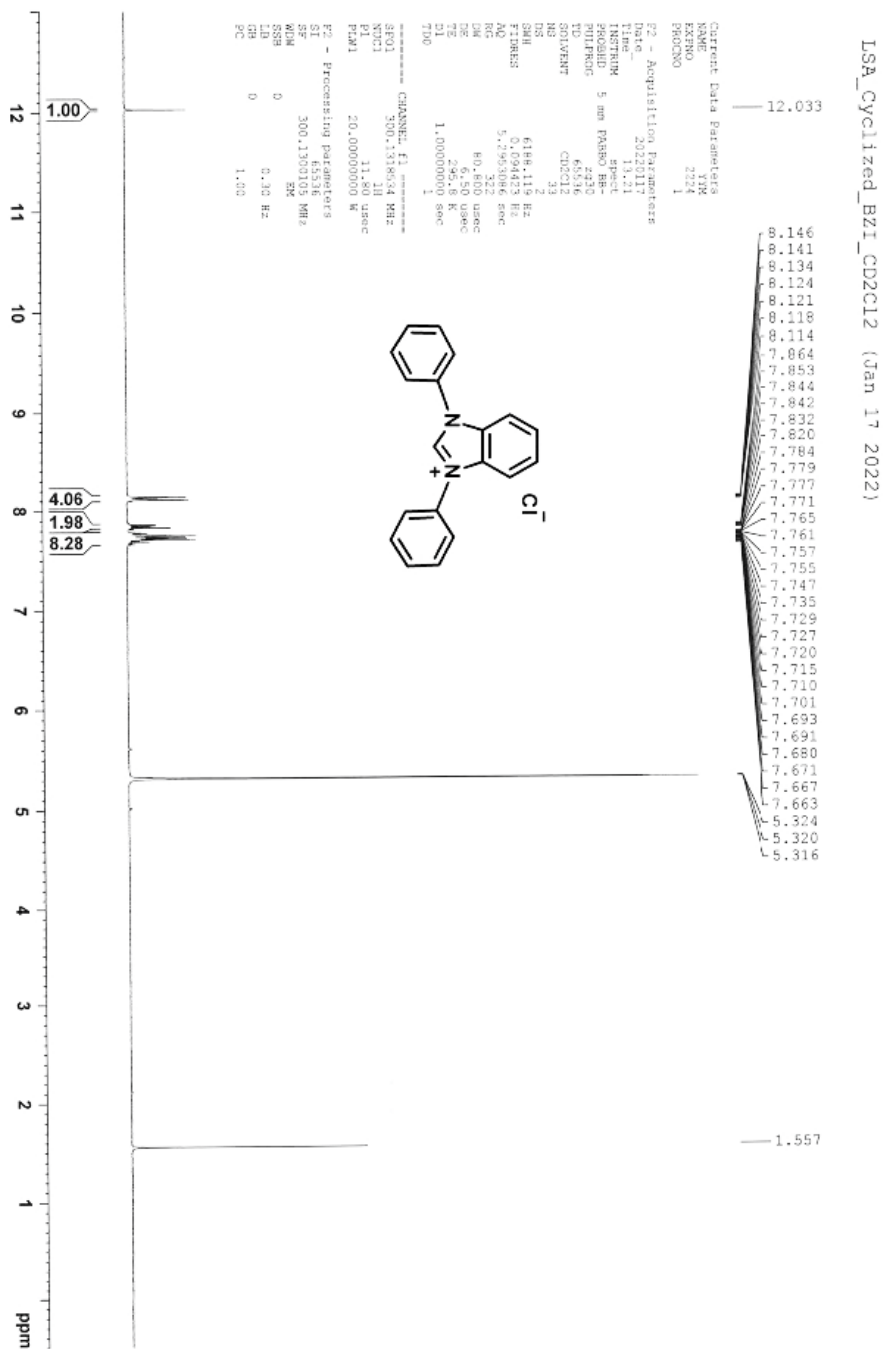


Fig. S16 ¹H NMR spectrum (300 MHz, CD₂Cl₂) of **2**.



```

Current Data Parameters
NAME      fe204-ehs-1a3
EXPNO     2
PROCNO    1

F2 - Acquisition Parameters
Date_     20220204
Time      16.40 h
INSTRUM   spect
PROBHD    2113652_0189 v
PULPROG   zgpg
TD         32768
SOLVENT   CDCl2
NS         1024
DS         4
SWH        31250.000 Hz
FIDRES     1.907349 Hz
AQ         0.5242890 sec
RG         16.2050
DM         16.000 usec
DE         26.30 K
TE         300.2 K
D1         3.0000000 sec
D11        0.03000000 sec
TDO        1
SFO1       125.7716224 MHz
NUC1       13C
P1         10.00 usec
PLM1       90.00000000 N
SFO2       500.1320005 MHz
NUC2       1H
CPDPRG12  waltz16
PCPD2     80.00 usec
PLM2     19.00000000 N
PLM12     0.30886899 N

F2 - Processing Parameters
SI         16394
SF         125.7571227 MHz
WDW        EM
SSB        0
LB         1.50 Hz
GB         0
PC         1.40
  
```

Fig. S17 $^{13}\text{C}\{^1\text{H}\}$ NMR spectrum (126 MHz, CD_2Cl_2) of 2.

[Mass Spectrum]
Data : FAB-D170 Date : 08-Feb-2022 15:58
RT : 0.10 min Scan# : (3,8)
Elements : C 100/0, H 100/0, N 10/0
Mass Tolerance : 10ppm, 5mmu if m/z < 500, 10mmu if m/z > 1000
Unsaturation (U.S.) : -0.5 - 30.0

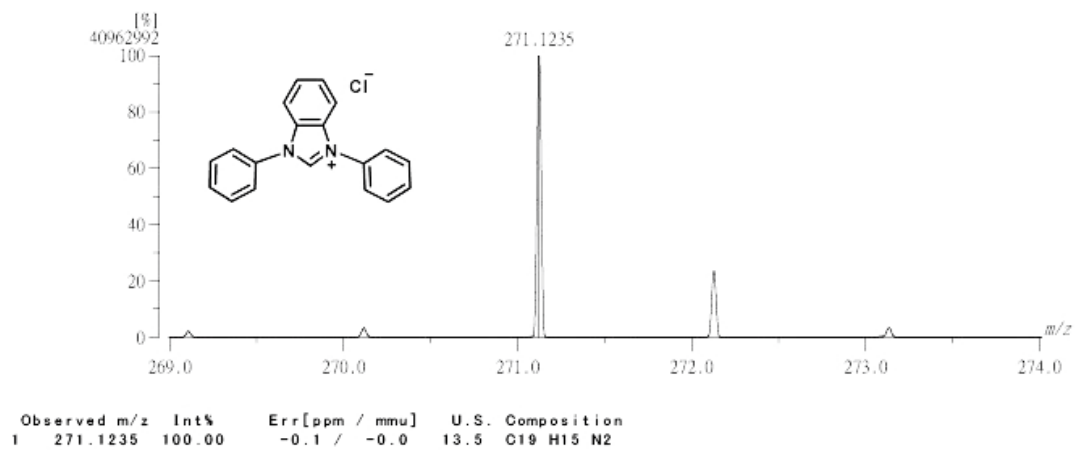


Fig. S18 High-resolution mass spectrum (FAB (*m*-NBA), positive) of **2**.

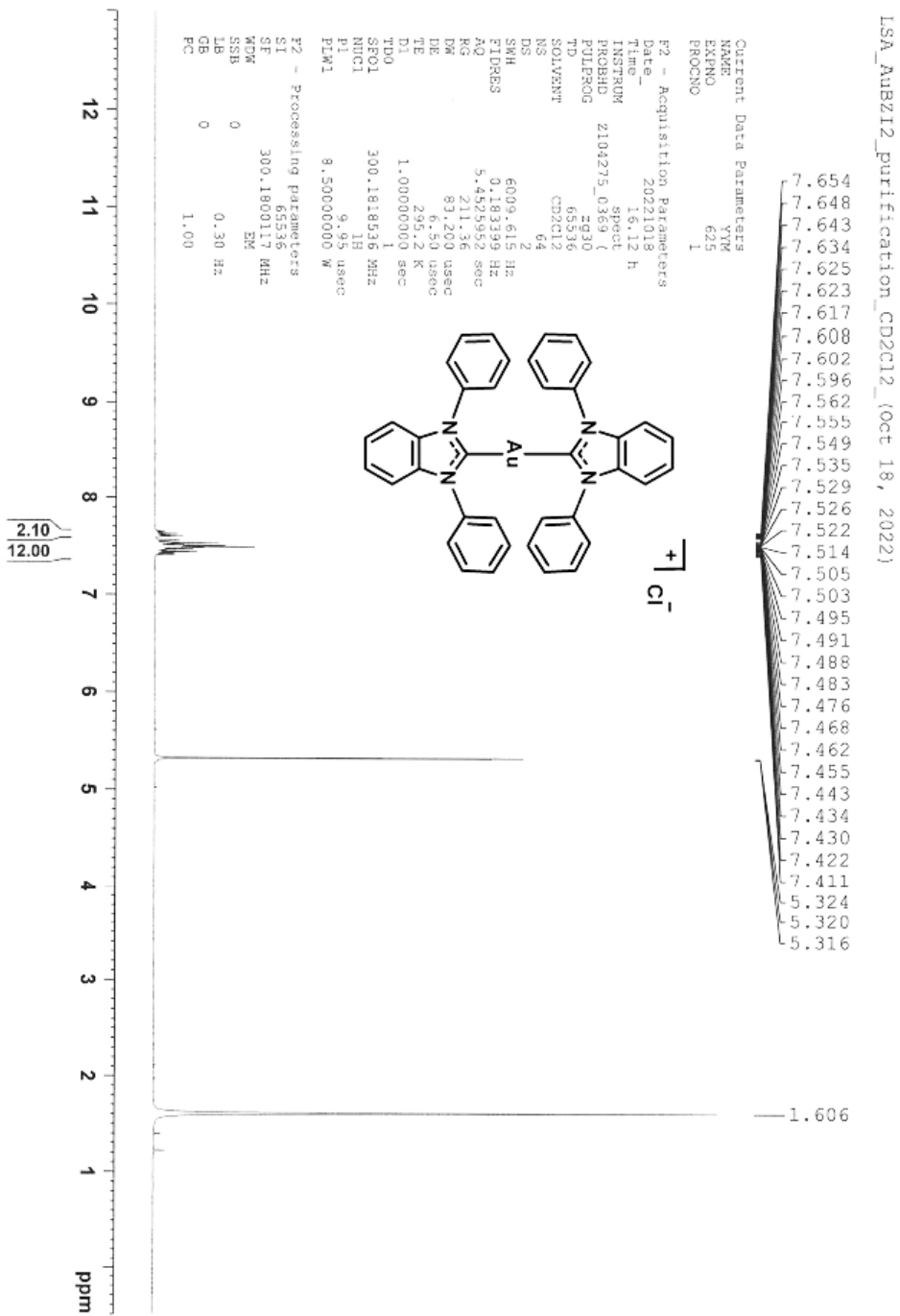


Fig. S19 ^1H NMR spectrum (300 MHz, CD_2Cl_2) of $[\text{Au}(\text{BZI})_2]\text{Cl}$.

[Mass Spectrum]
Data : FAB-D1050 Date : 04-Oct-2022 17:48
RT : 0.06 min Scan# : (2,7)
Elements : C 100/0, H 100/0, N 10/0, Au 1/0
Mass Tolerance : 10ppm, 5mmu if m/z < 500, 10mmu if m/z > 1000
Unsaturation (U.S.) : -0.5 - 40.0

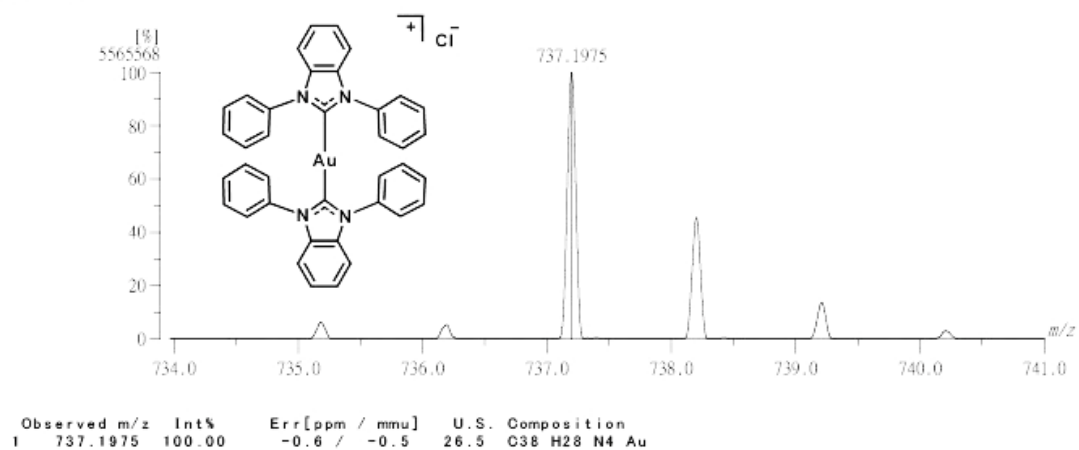


Fig. S21 High-resolution mass spectrum (FAB (*m*-NBA), positive) of [Au(BZI)₂]Cl.

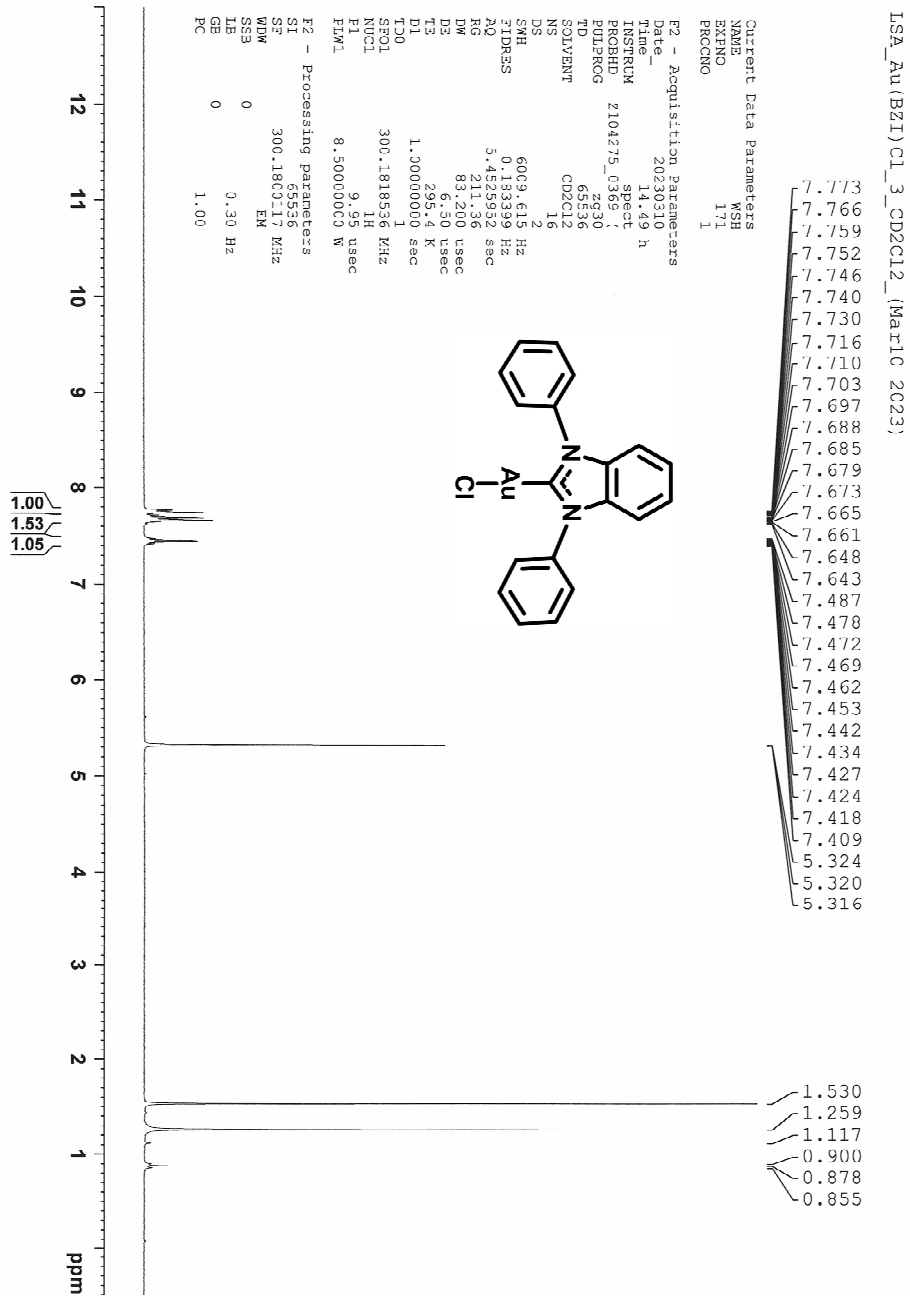


Fig. S22 ¹H NMR spectrum (300 MHz, CD₂Cl₂) of **3**.

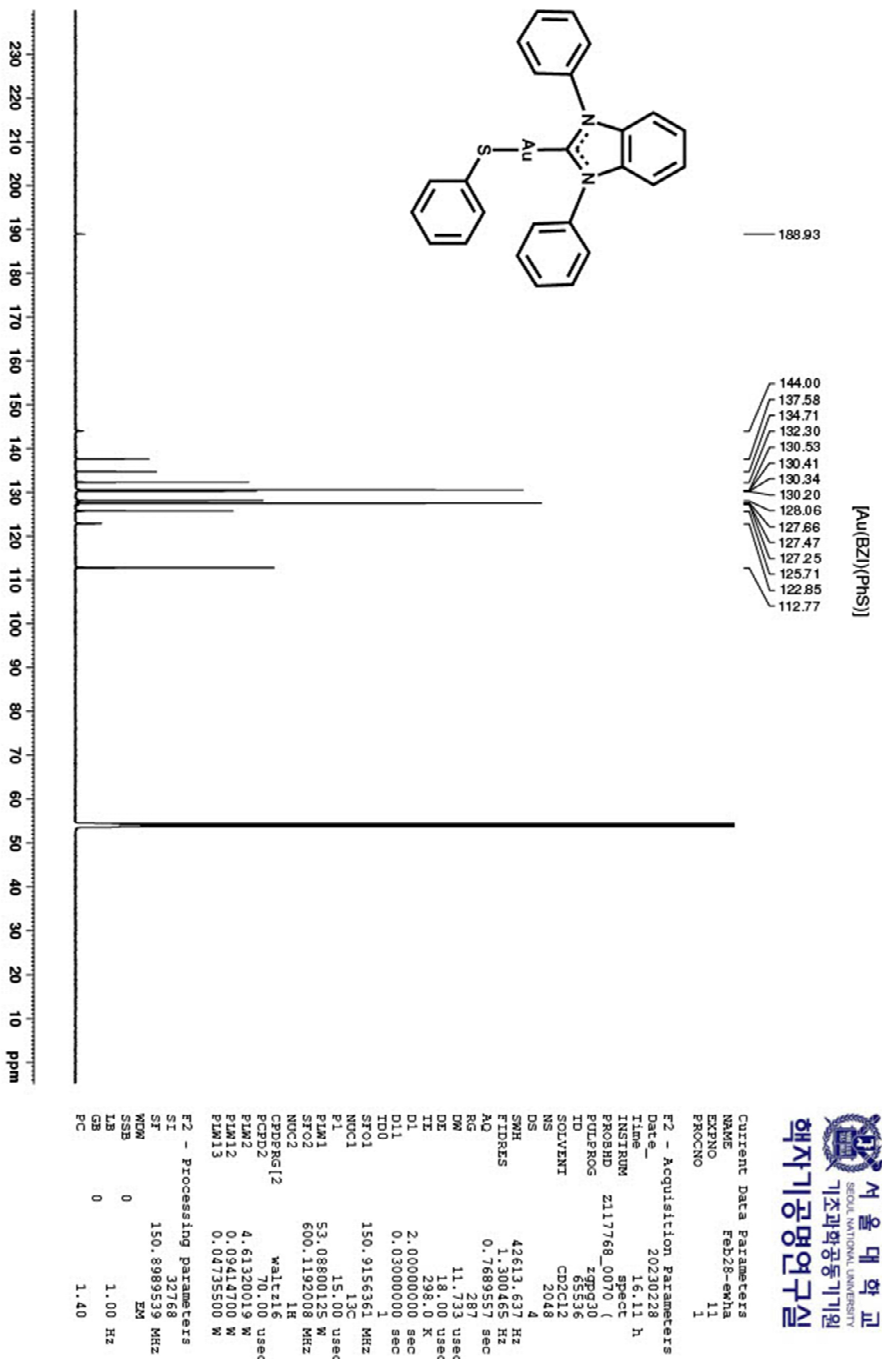
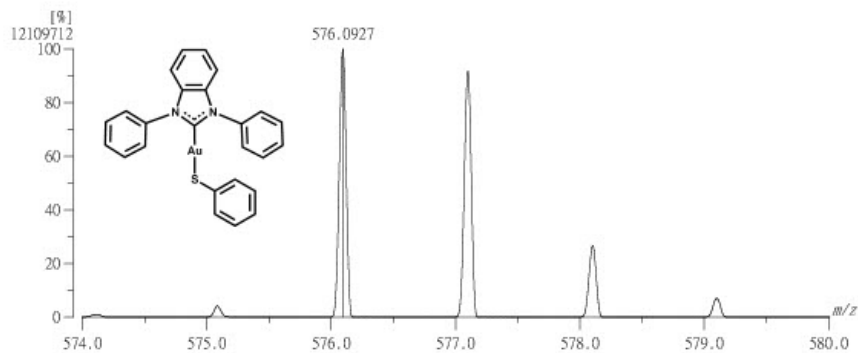


Fig. S24 $^{13}\text{C}\{^1\text{H}\}$ NMR spectrum (126 MHz, CD_2Cl_2) of $[\text{Au}(\text{BZI})(\text{PhS})]$.

[Mass Spectrum]
 Data : FAB-E541 Date : 02-Mar-2023 11:27
 RT : 0.00 min Scan# : (1,5)
 Elements : C 100/0, H 100/0, N 3/0, O 10/0, S 2/0, Au 1/0
 Mass Tolerance : 10ppm, 5mmu if m/z < 500, 10mmu if m/z > 1000
 Unsaturation (U.S.) : 10.0 - 25.0



Observed m/z	Int%	Err [ppm / mmu]	U. S.	Composition
1	576.0927	100.00	-0.6 / -0.4	24.5 C32 H18 N O10
2			+8.3 / +4.8	25.0 C33 H20 O8 S
3			-8.5 / -3.7	20.5 C29 H22 N O10 S
4			+4.8 / +2.8	21.5 C28 H22 N3 O7 S2
5			+2.5 / +1.4	21.0 C30 H24 O8 S2
6			+9.5 / +5.5	17.0 C25 H24 N2 O10 S2
7			+4.5 / +2.6	22.0 C28 H15 N2 Au
8			+9.2 / +5.3	17.5 C25 H17 N O3 Au
9			-5.7 / -3.3	13.0 C21 H19 N2 O5 Au
10			-1.3 / -0.8	18.0 C25 H19 N2 S Au
11			+3.3 / +1.9	13.5 C22 H21 N O3 S Au
12			-7.2 / -4.1	14.0 C22 H23 N2 S2 Au

Fig. S25 High-resolution mass spectrum (FAB (*m*-NBA), positive) of [Au(BZI)(PhS)].